

Thermochemistry for the Gas-Phase Ion-Molecule Clustering of CO_2^+CO_2 , SO_2^+CO_2 , $\text{N}_2\text{O}^+\text{N}_2\text{O}$, O_2^+CO_2 , NO^+CO_2 , $\text{O}_2^+\text{N}_2\text{O}$, and $\text{NO}^+\text{N}_2\text{O}$: Description of a New Hybrid Drift Tube/Ion Source with Coaxial Electron Beam and Ion Exit Apertures

Andreas J. Illies

Department of Chemistry, Auburn University, Auburn, Alabama 36849-3501 (Received: September 22, 1987)

A mass spectrometer ion source designed specifically to measure high-pressure gas-phase ion-molecule equilibria as a function of temperature was developed. The ion source has coaxial electron entrance and ion exit apertures. Ions move through the source at a constant velocity determined by a uniform electric field gradient which is controlled by overlapping drift guard rings. The transport properties of Ar^+ (mobility and diffusion) demonstrate that the effect of the electric field is negligible compared to thermal energies. Equilibria were investigated for the reactions forming the following gas-phase ion-molecule clusters: CO_2^+CO_2 , SO_2^+CO_2 , $\text{N}_2\text{O}^+\text{N}_2\text{O}$, O_2^+CO_2 , NO^+CO_2 , $\text{O}_2^+\text{N}_2\text{O}$, and $\text{NO}^+\text{N}_2\text{O}$. The measured enthalpies and entropies of reaction were used to determine the cluster ion enthalpies and entropies of formation at 298 K. The bond energies (from the enthalpies at 0 K) were determined to be for CO_2^+CO_2 , $D^\circ_0 = 15.9$ kcal/mol; for SO_2^+CO_2 , $D^\circ_0 = 10.2$ kcal/mol; for $\text{N}_2\text{O}^+\text{N}_2\text{O}$, $D^\circ_0 = 13.3$ kcal/mol; for O_2^+CO_2 , $D^\circ_0 = 9.8$ kcal/mol; for NO^+CO_2 , $D^\circ_0 = 8.6$ kcal/mol; for $\text{O}_2^+\text{N}_2\text{O}$, $D^\circ_0 = 10.8$ kcal/mol; and for $\text{NO}^+\text{N}_2\text{O}$, $D^\circ_0 = 7.7$ kcal/mol. The experimental entropies of reaction for the formation of $\text{O}_2^+\text{N}_2\text{O}$ and $\text{NO}^+\text{N}_2\text{O}$ are substantially less negative than those for O_2^+CO_2 and NO^+CO_2 . The entropy differences are large enough to suggest an inherent difference between the bonding or geometry for the ions bound to N_2O compared to those bound to CO_2 .

Introduction

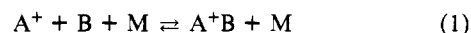
Gas-phase ion-molecule clusters are extremely interesting from both a practical and fundamental point of view. From the fundamental point of view, interest in these clusters arises since the bonding is intermediate between van der Waals and covalent bonding¹⁻⁴ and because of the analogies that are being drawn between ion-molecule clusters and intermediates in chemical catalysis.⁵ From a more practical point of view, research in this area has centered on the role that ion-molecule clusters play in the upper atmosphere, in solvation, in nucleation, and in high-energy environments such as flames, lasers, plasmas, and discharges.^{1-4,6}

Bonding between the two moieties in ion-molecule clusters ranges from nonrigid components held together predominantly by weakly directed electrostatic forces to more rigid moieties held together by a combination of electrostatic forces and varying amounts of orbital overlap (covalent bonding).⁷⁻⁹

Most thermochemical data on clusters come from ion-molecule equilibrium measurements or photoionization measurements and have been compiled by Keese and Castleman.³ Until recently very little was known about the detailed structure and bonding of the ion-molecule clusters because of the difficulties in generating large enough densities of the clusters for spectroscopic studies. However, in the past few years, much progress has been made with the development and application of a wide range of experimental techniques including photodissociation,^{1,3,6,7,11-13} pho-

toionization,^{2,3,8,14-16} collision-induced dissociation,^{11,17,18} and metastable reactions,¹⁷⁻²⁰ as well as the more traditional equilibrium methods.^{2,3,21}

As pointed out by Keese and Castleman³ and others,⁷ bond energies obtained from photoionization experiments can underestimate the energy if a considerable geometry change takes place upon ionization and if the adiabatic ionization is not sampled. In addition, photoionization experiments do not yield information on the entropy changes that occur. Equilibrium measurements, on the other hand, result in the enthalpy and entropy of reaction at the temperature of the measurement. The enthalpy and entropy of formation for the cluster molecule can then be determined and corrections applied to yield ΔH°_0 (the enthalpy at 0 K). For association reactions



the dissociation energy D°_0 of the cluster bond formed in the reaction is equivalent to ΔH°_0 of reaction.

In the present work a new variable-temperature high-pressure hybrid drift tube/ion source with axial electron entrance/ion exit apertures is described. The hybrid drift tube/ion source (referred to as HDT/IS or the ion source) was designed specifically to study gas-phase ion-molecule equilibrium reactions and is similar in concept to previously described ion sources.²²⁻²⁴ The temperature of the HDT/IS is variable, allowing equilibrium measurements as a function of the reaction temperature which result in van't Hoff plots and thus ΔH° and ΔS° of reaction.

(1) Illies, A. J.; Jarrold, M. F.; Wagner-Redeker, W.; Bowers, M. T. *J. Phys. Chem.* **1984**, *88*, 5204.

(2) Mark, T. D.; Castleman, A. W., Jr. *Adv. At. Mol. Phys.* **1985**, *20*, 66.

(3) Keese, R. G.; Castleman, A. W., Jr. *J. Phys. Chem. Ref. Data* **1986**, *15*, 1011.

(4) Castleman, A. W., Jr.; Keese, R. G. *Chem. Rev.* **1986**, *86*, 589.

(5) Alford, J. M.; Weiss, F. D.; Leaksonen, R. T.; Smalley, R. E. *J. Phys. Chem.* **1986**, *90*, 4480 and references cited therein.

(6) Jarrold, M. F.; Illies, A. J.; Wagner-Redeker, W.; Bowers, M. T. *J. Phys. Chem.* **1985**, *89*, 3269.

(7) Jarrold, M. F.; Misev, L.; Bowers, M. T. *J. Chem. Phys.* **1984**, *81*, 4369.

(8) Pratt, S. T.; Dehmer, P. M. *J. Chem. Phys.* **1983**, *78*, 6336.

(9) Illies, A. J.; McKee, M. L.; Schlegel, B. H. *J. Phys. Chem.* **1987**, *91*, 3489.

(10) Jarrold, M. F.; Illies, A. J.; Bowers, M. T. *J. Chem. Phys.* **1983**, *79*, 6086.

(11) Bowers, M. T.; Illies, A. J.; Jarrold, M. F. *Chem. Phys. Lett.* **1983**, *102*, 335.

(12) Jarrold, M. F.; Illies, A. J.; Bowers, M. T. *J. Chem. Phys.* **1984**, *81*, 222.

(13) Jarrold, M. F.; Illies, A. J.; Bowers, M. T. *J. Chem. Phys.* **1984**, *81*, 214.

(14) Ng, C. Y. *Adv. Chem. Phys.* **1983**, *52*, 263.

(15) Linn, S. H.; Ng, C. Y. *J. Chem. Phys.* **1981**, *75*, 4921.

(16) Erickson, J.; Ng, C. Y. *J. Chem. Phys.* **1981**, *75*, 1650.

(17) Illies, A. J.; Bowers, M. T. *Org. Mass Spectrom.* **1983**, *18*, 553.

(18) Stephan, K.; Mark, T. D. *Chem. Phys. Lett.* **1982**, *87*, 226.

(19) Illies, A. J.; Jarrold, M. F.; Bowers, M. T. *Int. J. Mass Spectrom. Ion Phys.* **1983**, *47*, 93.

(20) Illies, A. J.; Jarrold, M. F.; Bass, L. M.; Bowers, M. T. *J. Am. Chem. Soc.* **1983**, *105*, 5776.

(21) The body of literature on ion-molecule equilibrium is enormous; the reader is referred to the recent reviews cited and the references therein.

(22) Illies, A. J.; Meisels, G. G. *Anal. Chem.* **1980**, *52*, 325.

(23) Van Koppen, P. A. M.; Kemper, P. R.; Illies, A. J.; Bowers, M. T. *Int. J. Mass Spectrom. Ion Processes* **1983**, *54*, 263.

(24) Jennings, K. R., private communication.

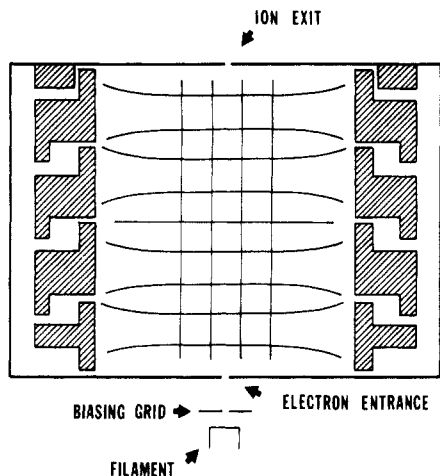


Figure 1. Schematic diagram of a cross section of the ion source. The equipotential lines (horizontal) and electric field lines (vertical) are shown.

In this paper experiments on known clusters performed to test the apparatus as well as experiments, results, and interpretation for some new ion-molecule clusters (see title) are presented. Important goals of this work are improving our understanding of chemical bonding in ion-molecule clusters and presenting reliable thermodynamic data for the clusters. The specific binding energies will be of great value in interpreting experiments on the clusters.

Experimental Section

The new HDT/IS was developed for use in a Du Pont 491B double-focusing mass spectrometer and is similar in concept to those previously developed by this author and others.²²⁻²⁴ The present design, however, has numerous improvements and warrants a detailed discussion. The HDT/IS is cylindrically symmetric about the direction of ion motion; a cross section is schematically shown in Figure 1. The HDT/IS has coaxial electron entrance and ion exit apertures; both apertures are circular holes, 0.013 cm in diameter. Ions, formed in the "rear" of the source by electron impact, move through a uniform potential gradient shaped by four overlapping drift guard rings (Figure 1).^{22,23} Each drift guard ring has four 1.0-mm holes drilled through the ring to allow gas flow and pressure equalization throughout the inner chamber of the source. The inside diameter of the drift guard rings is 1.9 cm, and the entire drift length is 2.0 cm, resulting in a relatively large diameter to drift length distance (0.95). This large ratio results in relatively flat equipotential electric field lines over the entire drift region. Figure 1 shows the equipotential lines determined empirically by using standard electrolytic plotting techniques. The flatness within the central portion of the HDT/IS means that the ion path through the drift region will be well-defined. A uniform potential drop over the drift region assures that, at high pressures where there are a sufficient number of collisions,^{22,23} the path of the ions will result from a combination of motion perpendicular to the equipotential lines and diffusion.

All metal parts (other than screws which are stainless steel) were machined from beryllium-copper alloy. Insulating parts are Teflon, Macor, or ceramic. A rhenium ribbon filament is used in the electron gun. The electron beam can be stopped by a biasing grid with a 1-mm hole 5 V positive with respect to the filament potential. The electron energy was always kept as low as possible (<22 eV) to reduce the relative population of excited states²³ as well as to ensure a point source of ion formation in the mobility and diffusion experiments.²²

To measure the van't Hoff plots, the ion source temperature must be varied; this is accomplished by flowing heated or cooled dry air through channels in the ion source block, resulting in a temperature range of approximately 80–540 K. Temperature measurements were made with a resistance probe (Pt 100 K 2015, Omega engineering) inserted into the HDT/IS block. The resistance probe is coated with "cry-con", a heat-conductive vacu-

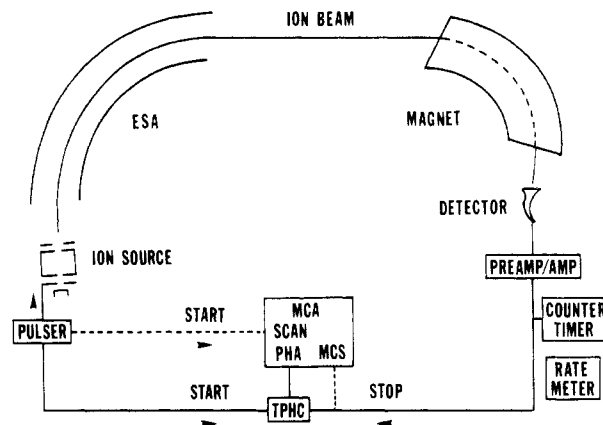


Figure 2. Schematic diagram of the instrument with pulsing and detection scheme. The solid lines show detection with the TPHC and PHA while the dotted line uses the MCS: TPHC, time-to-pulse height converter; PHA, peak height analyzer; MCS, multichannel scalar.

um-compatible grease, to ensure good thermal contact (Air Products and Chemicals). An Omega Model 661 resistance thermometer which is electrically floated at the ion block potential is used to measure the resistance.

Gas samples are introduced through an inlet consisting of three Granville-Phillips Series 203 leak valves which are connected to glass reservoirs (1–6 L) or gas cylinders and regulators via ultra-Torr fittings. The source gas pressure is measured with a MKS Baratron 170 sensor head capacitance manometer and a Type 270 B signal conditioner. Previous experiments²³ have shown that the inside diameter of the connecting line is sufficiently large between the source block proper and the lines at room temperature to avoid problems due to thermal transpiration.^{23,25} The useful pressure range of the HDT/IS is about 0.2–2.0 Torr, but in the present work pressures in the range 0.2–0.8 Torr were used. One of the reviewers has suggested that at the upper pressure limit significant adiabatic cooling could occur as the gas exits the ion exit aperture. We believe that this is not a concern for the present work.²⁶

The original geometry of the Du Pont ion optics was retained; however, modifications to the ion acceleration region were made to improve the differential pumping between the ion source housing and the analyzer region and to improve the pumping speed around the source and lenses. The pumping speed around the ion source was greatly improved by shortening the pumping conduit, reducing the number of bends in the conduit, and replacing the original 175 L/s diffusion pump with a Varian VHS-4 1200 L/s diffusion pump. Increased pumping results in reduced collision-induced dissociation in the acceleration region, which is a problem that must always be addressed when high-pressure mass spectrometry is used for equilibrium measurements.^{22,27,28}

(25) Dushman, S. *Scientific Foundation of Vacuum Technique*, 2nd ed.; Lafferty, J. M., Ed.; Wiley: New York, 1962.

(26) Adiabatic cooling can occur when gas exits an aperture if the mean free path is small compared to the hole size and cooperative flow takes place. Consideration of the ion exit orifice diameter (0.13 mm), thickness (0.13 mm), and the gas mean free path for our apparatus suggests that at the maximum useful pressure the mean free path is approximately 4 times greater than the "effective" orifice radius²⁵ while in fact at the highest pressure used in this work it is 13 times greater. Dushman²⁵ suggests that, in practice, effusive flow occurs when the mean free path to orifice radius ratio is greater than 2. Thus, on the basis of the kinetic theory of gases we would expect to be near the limit for cooperative flow (and hence adiabatic cooling) only in the worst possible case. Two experiments were carried out to test for cooperative flow and adiabatic cooling. In the first experiment the ion source was equilibrated at ambient temperature with the filament and temperature control systems off. Kr, also at ambient temperature, was then introduced at 1.8 Torr. The temperature was monitored for 1 h; no cooling was observed (± 0.3 °C). For the second experiment one must recognize if cooperative flow were taking place, collision-induced dissociation would occur in the ion acceleration region. Since the measured equilibrium constant is independent of total pressure, we expect that ion-molecule processes and collision-induced dissociation outside the ion source in the acceleration region are minimal. In summary, the author recognizes that adiabatic cooling could influence the results but believes that the evidence indicates that gas flow is effusive and not cooperative.

(27) Illies, A. J.; Meisels, G. G. *J. Phys. Chem.* **1982**, *86*, 1286.

Figure 2 shows the instrumental and electronic apparatus,^{22,23,29} which will only be briefly summarized here. The original Du Pont collector slit was slightly enlarged, resulting in flat-top peaks, which eliminates mass discrimination since in the flat region all ions of the selected mass are transmitted through the instrument.³⁰ Analog detection of the ion current uses the original Du Pont electronics with a Bell and Howell 5-131 recording oscillograph. Analog detection was used only to record mass spectra *but never for equilibrium measurements* since it is well-known that electron multipliers have different analog responses for different molecules. For instance, diatomic ions can produce currents that are nearly twice as large as monoatomic ions. To minimize discrimination from the electron multiplier, all quantitative experiments were carried out at high gain with fast ion counting. Under these conditions, one simply counts whether an ion is detected rather than how large a signal is produced. Specifically, ion counting is via a continuous dynode electron multiplier, an EG&G PARC Model 1182 fast amplifier/discriminator, Tennelec TC 534 counter/timer, Tennelec TC 536 ratemeter, EG&G Ortec 7100 multichannel analyzer (with both MCS and MCA capabilities), and finally an IBM-AT computer (Figure 2).

For pulsed experiments, the electron beam is turned on for 0.5–2 μs with a pulse from a Wavetec Model 191 pulse/function generator which is capacitance coupled to the biasing grid. Detection is through either of two modes. For short residence time distributions (less than 1000 μs) the trigger pulse starts an Ortec 567 time-to-amplitude converter and the ion pulse stops the converter. The output from the time-to-amplitude converter is processed by the multichannel analyzer in the PHA mode. For longer residence time distributions, the trigger pulse starts the sweep on the multichannel analyzer (MCS model) and all detected ions are stored in the appropriate channel as the sweep progresses (Figure 2, dotted line).

Simple statistics indicate that, for randomly spaced input pulses, some percentage of input counts will occur so closely spaced that they will be counted as one pulse instead of as two or more pulses (this is often referred to as pulse "pileup"). In the counting detection schemes used here the ion count rate was always kept low enough so that less than 0.1% ion loss would occur, i.e., less than 0.1% discrimination for the most intense ion beams.³¹

Gases used in these experiments were the purest that could be purchased from either Matheson Gas Products, Air Products, MG Industries Scientific Gases, or Alphagaz. Where necessary to remove trace water the gases were passed through a 3A molecular sieve which was as cold as compatible with the boiling point of the gas (down to 77 K). The gases were handled on a glass vacuum apparatus with a base pressure of about 1×10^{-6} Torr. The glass lines and glass containers were thoroughly baked out.

Results and Discussions

Mobility and Diffusion of Ar^+ in Ar. Measuring the mobility and diffusion of ions provides a good test for the operation of hybrid drift tube/ion sources such as the one described here. The drift velocity v_d of an ion packet is directly proportional to the electric field strength (E) and is given by

$$v_d = KE \quad (2)$$

(28) The effects of collision-induced dissociation of cluster ions on the equilibrium constants and hence ΔS° and ΔH° of reaction will be very similar to those of unimolecular dissociation described in detail by Sunner, J.; Kebarle, P. *J. Phys. Chem.* **1981**, *85*, 327.

(29) Sroka, G.; Chang, C.; Meisels, G. *J. Am. Chem. Soc.* **1972**, *94*, 1052.

(30) Illies, A. J.; Jarrold, M. F.; Bowers, M. T. *J. Am. Chem. Soc.* **1982**, *104*, 3587.

(31) No matter how short a pulse is and how fast the electronics is, some percentage of the pulses will occur so closely spaced that they will be detected as one. The percentage of randomly spaced pulses that is lost due to pile up is approximately given by

$$\% \text{ pulses lost} = (100)(\text{pulse rate})(\text{resolution})$$

In our apparatus the multichannel analyzer, the limiting device, is triggered by 50- μs pulses resulting in 0.1% loss at count rates of 2×10^4 counts/s.

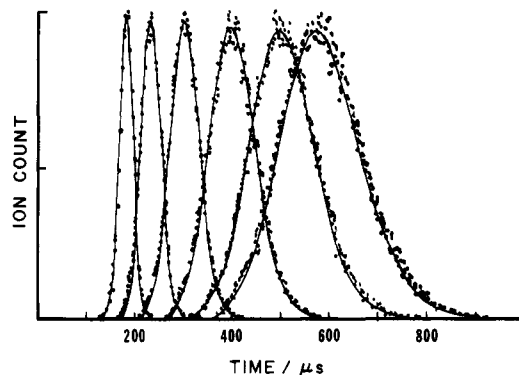


Figure 3. Experimental and calculated (eq 5) residence time distributions of Ar^+ in Ar at various of field strengths. The calculated lines fall directly on the experimental points. The pressure and temperature were 0.815 Torr and 416 K, respectively. The electric field decreases from left to right; in units of E/N they were 9.99, 11.31, 13.9, 18.7, 24.6, and 32.0 Td ($1 \text{ Townsend (Td)} = 10^{-17} \text{ V}\cdot\text{cm}^2$).

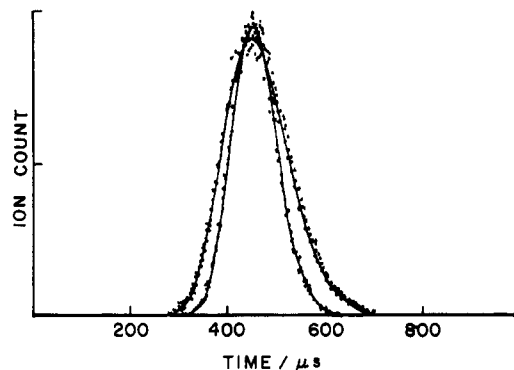


Figure 4. Residence time distributions at two different pressures showing the broadening due to increased diffusion at lower pressures. The agreement between the calculated and experimental distributions is excellent when the Einstein equation (eq 6) for the diffusion coefficients is used. The temperature was 444 K, and the field strength was 14.24 Td ($1 \text{ Td} = 10^{-17} \text{ V}\cdot\text{cm}^2$).

where the proportionality constant K is the mobility.^{22,23,32,33} Mobilities are thus determined from the ion source residence times t_{av} and the drift distance z according to the relation

$$K = v_d/E = (z/t)/E \quad (3)$$

Ion mobilities, however, are inversely proportional to the gas density; therefore, the reduced mobility K_0 is usually reported:

$$K_0 = K(P/760)(273/T) \quad (4)$$

where P is the pressure in Torr and T the temperature in degrees Kelvin.

The reduced mobility is usually measured as a function of the ratio of the electric field strength to the neutral gas number density, E/N . Under conditions of low E/N , the drift velocity of the ions gained from the electric field is small compared to thermal energies and the reduced mobility becomes independent of E/N .^{23,32,33} By extrapolating to zero E/N , the zero field mobilities are obtained. Figure 3 shows several residence time distributions for Ar^+ in Ar at various values of E/N , 416 K, and 0.815 Torr (hence constant N). The points in Figure 4 represent the experimental results. Within the error of the measurements, all the distributions in Figure 3 result in the same value for the reduced mobility, i.e., $K_0 = 1.31 \pm 0.08 \text{ cm}^2/(\text{V}\cdot\text{s})$. All the data in Figure 3 result in the same reduced mobility, implying that the low-field conditions have been met. The value for the reduced mobility of Ar^+ in Ar from this work ($K_0 = 1.31 \text{ cm}^2/(\text{V}\cdot\text{s})$) compares reasonably well

(32) McDaniel, E. W.; Mason, E. A. *The Mobility and Diffusion of Ions in Gases*; Wiley: New York, 1973.

(33) McDaniel, E. W. *Collision Phenomena in Ionized Gases*; Wiley: New York, 1964.

with previous reported values extrapolated to the same temperature ($K_0 = 1.3\text{--}1.4 \text{ cm}^2/(\text{V}\cdot\text{s})$).^{22,23,32,33}

It should be noted that the above discussion on the mobilities of ions holds true only for nonreactive ions. For ions involved in chemical reactions the residence time distributions differ from those for nonreactive systems; for instance, when equilibrium between two ions is established, the residence time distributions of the reactant and the product ions overlap exactly³⁴ (also see discussion and data to follow).

Meisels³⁵ has discussed the calculation of residence time distributions for various source geometries. For a point source of ions ($x = y = z = 0$ at time $t = 0$) and a circular ion collection aperture of radius r_c , the collected ion current is given by

$$i_c(r_c, t, z) = \frac{n_0}{4} \left(\frac{v_d + \frac{z}{t}}{(\pi D_0 t)^{1/2}} \right) \exp\left(-\frac{(z - v_d t)^2}{4 D_0 t}\right) \left(1 - \exp\left(\frac{-r_c^2}{4 D_0 t}\right) \right) \quad (5)$$

where D_0 is the diffusion coefficient, t is time, and all other terms have already been defined. The lines in Figure 3 represent the calculated residence time distributions where the diffusion coefficient used to fit the experimental data ($62 \text{ cm}^2/\text{s}$) was determined using the Einstein equation^{32,33}

$$D_0 = K_0 T^2 (2.39 \times 10^{-4}) / P \quad (6)$$

and the experimentally measured reduced mobility. In previous experiments by Illies et al.²² and Van Koppen et al.²³ using similar HDT/IS's it was found that, in order to match the experimental results, diffusion coefficients slightly larger than those given by the Einstein relationship but smaller than those predicted for ambipolar diffusion^{32,33} were required

$$D_a = K_0 T^2 (4.79 \times 10^{-4}) / P \quad (7)$$

Ambipolar diffusion is the diffusion of positive ions in the presence of electrons. Since electrons are much more mobile than ions, the electrostatic forces between the electrons, which diffuse faster, and the ions result in broader residence time distributions for the ions. It was suggested that such a dependence might be expected under the conditions in the ion source.^{22,23} The present experiments indicate that the previous interpretation was incorrect. Actually, since a drift field is present inside the ion source, ions will drift toward the ion exit slit while electrons will drift toward the rear of the source and will be quickly annihilated at the source walls. Thus one would expect that the ion packet might only be slightly "blown up" due to a very small contribution of ambipolar diffusion at short times.

The author feels that a more feasible explanation for the wider experimental residence time distributions observed by previous workers is that the equipotential lines inside the ion sources were not as flat and parallel as previously thought and that the ion packet was sprayed out in the source by the imperfections in the electric fields. In addition, ion collection in the present experiment is through a circular hole which samples only those ions in the center of the source rather than through a slit which will sample ions nearer the edges of the source.

Figure 4 shows two distributions which further test the ion drift properties. Here the mobility for the two distributions is kept constant but the pressure is varied. As can be seen in eq 6, the diffusion constant depends inversely upon the neutral gas pressure even under conditions of constant reduced mobility and temperature. As expected, the distribution collected at lower pressure is broader than that collected at higher pressure. Again, the curves represent distributions calculated with eq 5 and the diffusion coefficients calculated with the Einstein relation (eq 6). The

author believes that a match between experimental distributions and calculated distributions by using the Einstein diffusion coefficient is probably a good test for flat equipotential and electric field lines within the ion source. The ion source described here achieves flat equipotential lines in two ways: (1) the ratio between the inside diameter of the drift guard rings and the total drift distance is large and (2) more drift guard rings are used to cover a drift distance comparable to that used in other instruments.^{22,23}

Ion-Molecule Clustering Equilibrium Reactions. An important goal for this work is the study of gas-phase ion-molecule clustering equilibrium reactions. The heat of reaction ΔH° and the entropy of reaction ΔS° are derived from temperature studies of the equilibrium constant K_{eq} which result in the familiar van't Hoff equation

$$-RT \ln K_{eq} = \Delta G^\circ = \Delta H^\circ - T\Delta S^\circ \quad (8)$$

This equation is in fact only applicable for the case where ΔC_p (the difference in heat capacity between products and reactants) is zero. For real reactions ΔC_p will not be zero; hence eq 8 is approximate. In fact, ΔC_p is usually small and the temperature range over which experiments are carried out is not very large, resulting in straight lines for the experimentally observed data. Equilibrium studies using the van't Hoff equation have resulted in a great deal of reliable thermodynamic data for all types of ion-molecule reactions.^{2,3,21,23}

For the equilibrium reaction presented in eq 1 the equilibrium constant is given by

$$K_{eq} = [A^+B] / [A^+][B] \quad (9)$$

where the ionic and neutral species are expressed in units of concentration. If the ion current is proportional to the ion concentration, then $[A^+] = x_a(i_{A^+})$ where x_a is a proportionality constant and i_{A^+} is the measured ion current. A similar term applies for the cluster species; $[A^+B] = x_{ab}(i_{A^+B})$. One can then write the equilibrium constant as

$$K_{eq} = (x_{ab})(i_{A^+B}) / (x_a)(i_{A^+})[B] \quad (10)$$

In the absence of instrumental mass discrimination, the proportionality constants x_a and x_{ab} will be the same and will thus cancel, leaving

$$K_{eq} = (i_{A^+B}) / (i_{A^+})[B] \quad (11)$$

In eq 11 only the reactant ion (i_{A^+}) and product ion (i_{A^+B}) currents and the neutral concentration $[B]$ are required to calculate the equilibrium constant. To reemphasize, this equation is only valid in the absence of instrumental mass discrimination. Each individual instrumental apparatus should therefore be examined for possible mass discrimination.

When equilibrium is established in a HDT/IS such as that used in this work, the average drift properties of both ions involved in the equilibrium are the same. The charges that are transmitted through the mass spectrometry and finally detected undergo many switching reactions as they travel through the source drift region to the exit slit. This results in identical residence time distributions for both ions.^{34,36,37} Hence, if discrimination of ions should occur before exiting the source, it will be the same for all ions involved in the equilibrium and the effects will cancel. Discrimination through the mass spectrometer itself and of the detection system was discussed under Experimental Section. Finally, on the topic of discrimination the reader should be reminded that if discrimination does occur and if the fraction is independent of the experimental temperature, it will affect only the intercept of the van't Hoff plot (which yields ΔS°) and not the slope (which yields ΔH°). That is, the van't Hoff equation (eq 8) becomes

$$\ln K_{eq(\text{measured})} = -\Delta H^\circ / RT + \Delta S^\circ / R + \text{Disc} / R \quad (12)$$

(34) Chang, C.; Sroka, G. J.; Meisels, G. G. *J. Chem. Phys.* **1971**, *55*, 5154.

(35) Chang, C.; Sroka, G. J.; Meisels, G. G. *Int. J. Mass Spectrom. Ion Phys.* **1973**, *11*, 367.

(36) Meisels, G. G.; Sroka, G. J.; Mitchum, R. K. *J. Am. Chem. Soc.* **1974**, *96*, 5045.

(37) Meisels, G. G.; Mitchum, R. K.; Freeman, J. R. *J. Phys. Chem.* **1976**, *80*, 2845.

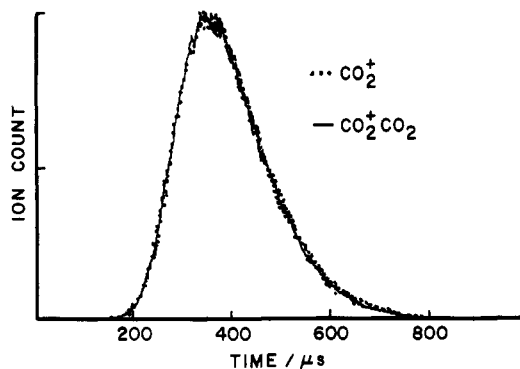


Figure 5. Residence time distributions for CO_2^+ (points) and CO_2^+CO_2 (line). The two distributions are essentially the same, showing that equilibrium was achieved. The temperature was 446 K and the electric field was 10.25 Td (1 Td = 10^{-17} V·cm²).

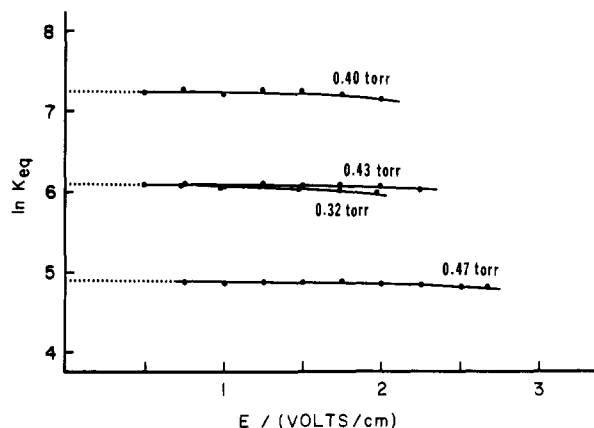
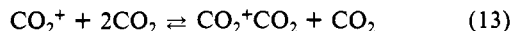


Figure 6. Plots of $\ln K_{\text{eq}}$ vs E for the CO_2^+CO_2 equilibrium system. The plots demonstrate that the measured equilibrium constant is independent of both the ion source pressure and the electric field at low field strengths and relatively high pressures. The temperatures were from top to bottom 468, 502, and 544 K.

where Disc is the discrimination which contributes to the intercept and will thus lead to misleading information on the entropy of reaction while the slope of the equation is unaffected and results in the correct enthalpy of reaction.

CO_2^+CO_2 . We have chosen to study a well-documented ion-molecule clustering reaction, the formation of CO_2^+CO_2 by the reaction



as a test equilibrium system.^{15,23,38-41} Figure 5 shows two residence time distributions; the points are for CO_2^+ and the line for CO_2^+CO_2 . Clearly, within the error limits and the limits of statistical noise, the two distributions are the same, implying that the system is at equilibrium under conditions at which the distributions were collected.

In addition to these pulsed experiments, continuous experiments (with the filament in the dc mode) were performed to test whether equilibrium was established. In the continuous experiments, the equilibrium constant was measured as a function of ion source pressure and ion extraction voltage (E/N). Typical plots of the natural logarithm of the measured equilibrium constant as a function of E/N are shown in Figure 6 at various temperatures and pressures. The experimental equilibrium constant is independent of E/N at the lower end of the E/N range measured, suggesting that the translational energy gained by the ions inside the source is negligible compared to thermal energies; thus true

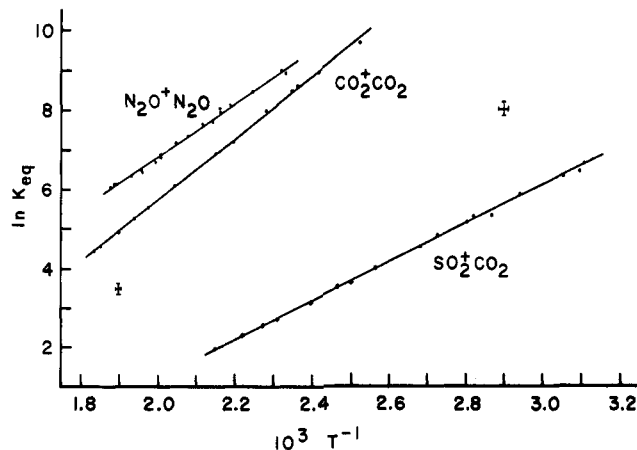


Figure 7. The van't Hoff plots for the association reactions for formation of $\text{N}_2\text{O}+\text{N}_2\text{O}$, CO_2^+CO_2 , and SO_2^+CO_2 .

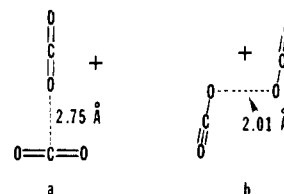
thermal equilibrium conditions were attained. The absence of a pressure dependence at low fields indicates that equilibrium was attained and that discrimination due to collision-induced dissociation of the cluster ion was not taking place.^{27,28}

Equilibrium measurements such as those shown in Figure 6 were repeated at various temperatures between 404 and 560 K. The van't Hoff plot with all the experimental data is shown in Figure 7. The line through the experimental points is the result of a linear regression. From this we find the thermodynamic data at 483 K (the mid temperature point) $\Delta H^\circ = -15.5 \pm 0.4$ kcal/mol and $\Delta S^\circ = -18.6 \pm 0.9$ cal/(mol·K). The errors are twice the standard deviation of the slope and the intercept from the linear regression. These numbers are in excellent agreement with previously reported values from thermodynamic measurements,^{3,23,39,40} however, the experimental bond energy resulting from photoionization experiments is substantially lower.^{3,15,39}

The bond dissociation energy D°_0 can be estimated by correcting for the differences in the heat capacity ΔC_p between reactants and products

$$\Delta H_0 = \Delta H_T - \int_0^T \Delta C_p(T) dT \quad (14)$$

The temperature corrections require knowledge of the molecular structure (rotational constants, vibrational frequencies, and electronic degeneracies), but this spectroscopic data is only rarely available for the cluster ion and usually must be estimated. Recent theoretical calculations⁹ on the structure of the CO_2^+CO_2 cluster were not able to conclusively arrive at a single most probable structure for the ion cluster. The authors suggested that structure **a** might be the lowest energy form but structure **b** could not be ruled out.



We have assumed structure **a** and used estimated parameters based upon the data in ref 9 and 20 to approximate the enthalpy of reaction at 0 K. The parameters and method used to estimate the thermodynamic values are discussed in the Appendix and are presented in Table II. The heat capacity correction term for the enthalpy is small and results in $D^\circ_0 = 15.9$ kcal/mol. The entropy and enthalpy of formation of the cluster estimated at 298 K are presented in Table I.

It has been pointed out that photoionization experiments can underestimate the bond dissociation energy of an ion if a large geometry change occurs upon ionization and hence the adiabatic ionization transition is not detected.^{3,6,9} This seems to be the case for the CO_2^+CO_2 system. Recent ab initio calculations⁹ and

(38) Jones, G. G.; Taylor, J. W. *J. Chem. Phys.* **1978**, *68*, 1767.

(39) Rakshit, A. B.; Warnek, P. *Int. J. Mass Spectrom. Ion Phys.* **1980**, *35*, 23.

(40) Headley, J. V.; Mason, R. S.; Jennings, K. R. *J. Chem. Soc., Faraday Trans. 1* **1982**, *78*, 933.

(41) Meot-Ner, M.; Field, F. H. *J. Chem. Phys.* **1977**, *66*, 4527.

TABLE I: Thermodynamic Results from This Work^a

| | cluster | | | | | | |
|--|----------------------------------|----------------------------------|-----------------------------------|---------------------------------|--------------------|----------------------------------|---------------------|
| | CO ₂ +CO ₂ | SO ₂ +CO ₂ | N ₂ O+N ₂ O | O ₂ +CO ₂ | NO+CO ₂ | O ₂ +N ₂ O | NO+N ₂ O |
| $\Delta H_{T, \text{react}}^{\circ}$ ^b | -15.5 ± 0.4 | -9.6 ± 0.2 | -13.1 ± 0.8 | -9.6 ± 0.3 | -8.5 ± 0.3 | -10.7 ± 0.4 | -7.7 ± 0.1 |
| D_0° ^c | 15.9 | 10.2 | 13.3 | 9.8 | 8.6 | 10.8 | 7.7 |
| $\Delta H_{T, \text{cluster}, 298}^{\circ}$ ^c | 114 | 110 | 324 | 176 | 134 | 289 | 264 |
| $\Delta S_{T, \text{react}}^{\circ}$ ^b | -18.6 ± 0.9 | -16.5 ± 0.7 | -12.4 ± 1.7 | -18.9 ± 0.6 | -18.0 ± 0.9 | -15.3 ± 1.0 | -14.9 ± 0.3 |
| $S_{T, \text{cluster}, 298}^{\circ}$ ^c | 85 | 94 | 92 | 86 | 80 | 87 | 85 |
| T | 483 | 394 | 481 | 361 | 336 | 410 | 307 |
| ΔIP^d | 0 | 1.43 | 0 | 1.710 | 4.519 | 0.835 | 3.644 |
| ΔH^e | -13.6 | | -13.1 | <-10.6 | <13.8 | | |
| | -16.2 | | | (-10.5) ^f | | | |
| | -15.8 | | | >-21.4 | | | |
| | -17 | | | -11.0 | | | |
| | -15.6 | | | | | | |
| ΔS^e | -21.1 | | | (-20.7) ^f | | | |
| | -22.8 | | | -21.7 | | | |
| | -19.1 | | | | | | |

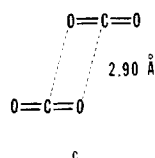
^aEnthalpies and bond dissociation energies are in kcal/mol. Entropies are in cal/(mol·K). Temperatures are in degrees Kelvin. Ionization differences are in eV. ^bExperimental result. ^cEstimated from the experimental results; see Results and Discussion and the Appendix. ^dThe difference in the ionization potentials for the two moieties in the cluster. IP's are from ref 50. ^eFrom the recent compilation by Keese and Castleman (ref 3). ^fData arrived at indirectly by switching reactions (see ref 3).

TABLE II: Input Parameters Used in the Entropy and Heat Capacity Corrections for CO₂+CO₂^{a,b}

| | CO ₂ ⁺ | CO ₂ | CO ₂ +CO ₂ |
|--|------------------------------|-----------------|----------------------------------|
| ν , cm ⁻¹ | | 1388 | 1388 |
| | | 667 (2) | 667 (2) |
| | | 2349 | 2349 |
| | 1230 | | 1230 |
| | 519 (2) | | 519 (2) |
| | 1475 | | 1475 |
| | | | 400 |
| | | | 140 |
| | | | 80 (2) |
| | | | 35 |
| $I_A I_B I_C$, ^c amu | | | 5691000 |
| g_i | 2 | 2 | 2 |
| r , ^c Å | | | 2.3 |
| angle, ^c deg | | | 110 |
| $S_{T, 298}^{\circ}$, cal/(mol·K) | 53.06 | 51.06 | |
| $\Delta H_{T, 298}^{\circ}$, kcal/mol | 224 ^d | -94.05 | |

^aParameters are defined in the text and in the Appendix. ^bData are from the JANAF tables. ^cEstimated. ^dEstimated using data from ref 50.

spectroscopic experiments⁴² on the neutral CO₂ dimer (van der Waals molecule) suggest that the most stable form is c.



In the present case, ionization from c to either a or b requires a substantial rearrangement. Although c and b appear to be similar in shape (a simple translation will result in the reorganization), the rearrangement involves a large change in the distance between the two moieties. Rearrangement from c to a clearly involves a large change in molecular orientation along what can be described as a vibrational degree of freedom. The fact that the photoionization results for the bond energy are lower than the results from equilibrium experiments (11.8 kcal/mol (ref 15) vs 19.9 kcal/mol (this work)) cannot be used to rule out either structure a or b for CO₂+CO₂.

In contrast to SO₂+CO₂, N₂O+N₂O, O₂+N₂O, and NO+N₂O still to be discussed, an internal rotation if not necessary in order

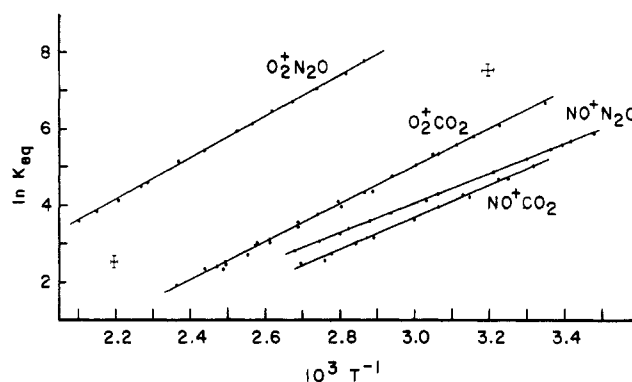
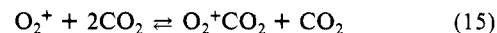


Figure 8. The van't Hoff plots for the association reactions for formation of O₂+CO₂, NO+CO₂, O₂+N₂O, and NO+N₂O.

to simulate the entropy for CO₂+CO₂, suggesting that a might be the observed structure since b is expected to have an internal rotation around the O-O bond (see further discussion later in this paper). It is unfortunate that the entropy is not more sensitive to the molecular structure, hence allowing more positive input into the question of which molecule represents the lowest energy form. A more definitive answer cannot be provided until further spectroscopic data are available.

O₂+CO₂ and NO+CO₂. O₂+CO₂ and NO+CO₂ clusters were made by introducing traces of either O₂ or NO into research grade CO₂. In each case electron impact produces CO₂⁺ which undergoes charge-transfer reaction with the trace component, resulting in the cation involved in the equilibrium reactions



The usual tests for equilibrium described in the previous sections were performed, resulting in the van't Hoff plots shown in Figure 8 and the thermodynamic results listed in Table I. The experimental enthalpies of reaction are -9.6 and -8.5 kcal/mol and the entropies of reaction -18.9 and -18.0 cal/(mol·K) for O₂+CO₂ and NO+CO₂, respectively. Agreement between the results from this work and the literature^{3,43-46} for O₂+CO₂ is fairly good (Table

(44) Beyer, R. A.; Vanderhoff, J. A. *J. Chem. Phys.* **1976**, *65*, 2313.

(45) Yamabe, S.; Hirao, K.; Hiraoka, K. *J. Chem. Phys.*, in press.

(46) Rakshit, A. B.; Warneck, P. *Int. J. Mass Spectrom. Ion Phys.* **1981**, *40*, 135.

(47) Kimura, K.; Katsumata, S.; Achiba, Y.; Yamazaki, T.; Iwata, S. *Handbook of He I Photoelectron Spectra of Fundamental Organic Molecules*; Japan Scientific Societies: Tokyo; Halsted: New York, 1981.

(42) Jucks, K. W.; Huang, Z. S.; Dayton, D.; Miller, R. E.; Lafferty, W. *J. J. Chem. Phys.* **1987**, *86*, 4341.

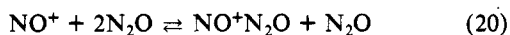
(43) Dotan, I.; Davidson, J. A.; Fehsenfeld, F. C.; Albritton, D. L. *J. Geophys. Res.* **1978**, *83*, 4036.

I) except for the early result of Meot-Ner and Field,^{3,41} which seems to be in error. Only a limit on the enthalpy of reaction for formation of NO^+CO_2 has been reported (<13.8 kcal/mol); the present result is in agreement with this limit.³

Bond energies were estimated by using the experimental entropy and a treatment analogous to that described for CO_2^+CO_2 in the previous section and in the Appendix: the energies are 9.8 and 8.6 kcal/mol for O_2^+CO_2 and NO^+CO_2 , respectively. No structural information was deduced from the entropy and the statistical mechanical calculations for these ions.

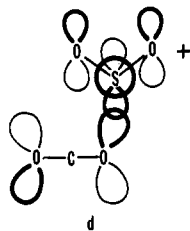
NO^+ is an unusual ion in that it has an even number of electrons and that the HOMO is filled, while O_2^+ is a radical cation. In spite of this, when the entropy and enthalpy of reaction for clustering with CO_2 are considered, both ions behave similarly (Table I). This trend was also observed to a lesser extent for NO^+ and O_2^+ binding to N_2O (see next section).

SO_2^+CO_2 , $\text{N}_2\text{O}^+\text{N}_2\text{O}$, $\text{O}_2^+\text{N}_2\text{O}$, and $\text{NO}^+\text{N}_2\text{O}$. The clusters in the subheading were studied by via the appropriate equilibrium reactions



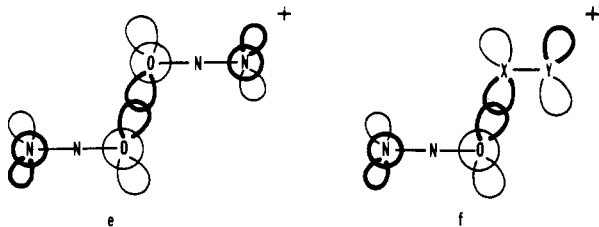
The van't Hoff plots are shown in Figures 7 and 8, and the thermodynamic results are presented in Table I. As demonstrated by the table, the entropies of reaction for formation of these clusters are higher (more positive) than expected for association reactions of this sort. In order to match the experimental entropies it was necessary to include an internal rotation in the statistical mechanical calculations for each cluster ion.

The author is not aware of any previous work on the SO_2^+CO_2 cluster ion. In the absence of ab initio calculations, consideration of a simple picture of chemical bonding often can be useful. For SO_2^+CO_2 , the HOMO/LUMO model predicts that electron transfer from the HOMO of CO_2 to the LUMO of SO_2^+ is responsible for the bonding. It is not possible to definitively arrive at a structure for SO_2^+CO_2 ; however, the requirement for an internal rotation in the molecule would rule out a "T"-shaped C_{2v} geometry with one of the oxygens on the neutral CO_2 bound to the sulfur atom of the cation. **d** shows a molecular structure which



allows for an internal rotation about the O-S bond and is consistent with the molecular orbitals calculated by Kimura et al.⁴⁷

For $\text{N}_2\text{O}^+\text{N}_2\text{O}$, $\text{O}_2^+\text{N}_2\text{O}$, and $\text{NO}^+\text{N}_2\text{O}$ neither T-shaped nor linear molecules allow for internal rotation. In addition, a T-shaped arrangement is not expected for $\text{N}_2\text{O}^+\text{N}_2\text{O}$ since the HOMO on N_2O has very little electron density on the central N atom.⁴⁷ Thus on the basis of the experimental entropy the author suggests that the molecular structures might be represented by **e** and **f** (or similar arrangements with different conductivity),



which allow for internal rotational degrees of freedom about the

bond joining the two moieties. In **f** XY^+ is either O_2^+ or NO^+ .

The binding energy of $\text{N}_2\text{O}^+\text{N}_2\text{O}$ has been reported by Linn and Ng to be 13.1 ± 0.9 kcal/mol.^{3,15} This number was determined from the photoionization threshold and the estimated bond energy for the neutral $\text{N}_2\text{ON}_2\text{O}$ van der Waals cluster (0.46 kcal/mol). As with most clusters, one expects that substantial rearrangement might take place upon ionization of the van der Waals clusters, implying that the adiabatic ionization transition might be weak due to the poor Franck-Condon overlap. The heat of reaction from this work was found to be -13.1 ± 0.8 kcal/mol at 481 K, which when corrected to 0 K results in a binding energy of 13.3 kcal/mol. This experimental result is in excellent agreement with the previously measured value from photoionization of the neutral cluster. Thus, it seems that in spite of the gradual photoionization onset, the adiabatic transition was sampled in the photoionization experiments.¹⁵

It would be interesting to have available photodissociation kinetic energy release data for the clusters presented in this section since, on the basis of a linear or symmetric T-shaped structure, one would expect very little rotational excitation upon dissociation (a simple impulsive picture for the photodissociation^{7,10,48} would predict a small rotational torque on either moiety with appreciable vibrational excitation because the dissociation forces are along the dissociating bond). On the other hand, the same impulsive model would predict considerable rotational and very little vibrational excitation for arrangements such as **e** and **f**. It is possible that with the aid of kinetic energy release distributions^{7,11-13} one could strengthen or disprove the predictions on the molecular structures presented here.

Summary and Conclusions

Excellent agreement between the calculated and experimental drift properties of Ar^+ in Ar show that the ion source described here operates well as a small drift tube. Measurements of the enthalpy and entropy of reaction by equilibrium techniques of the well-known ion-molecule equilibrium reaction for the formation of the CO_2^+CO_2 cluster ion (reaction 13) are in excellent agreement with literature values. These tests of the newly assembled apparatus demonstrate the reliability of the instrument.

The enthalpy and entropies at the appropriate temperatures for the reactions resulting in cluster formation are reported in Table I. Temperature corrections were made with statistical thermodynamics to estimate the cluster enthalpies and entropies of formation at 298 K and the bond energies at 0 K. The entropies of reaction are appreciably less negative for $\text{N}_2\text{O}^+\text{N}_2\text{O}$, SO_2^+CO_2 , $\text{O}_2^+\text{N}_2\text{O}$, and $\text{NO}^+\text{N}_2\text{O}$ than for CO_2^+CO_2 , O_2^+CO_2 , and NO^+CO_2 . Statistical mechanical calculations suggest that this may be due to internal rotational degrees of freedom that are active for the former ions and not active for the latter ions, hence, that there is an inherent difference between the bonding and/or geometry for the two sets of ions. This is especially noticeable for $\text{O}_2^+\text{N}_2\text{O}$ and $\text{NO}^+\text{N}_2\text{O}$ vs O_2^+CO_2 and NO^+CO_2 .

The nature of the bond between the two moieties in ion-molecule clusters is extremely interesting. Binding interactions range from weakly spatially directed electrostatic forces such as proposed for the binding of a variety of ligands to the alkali-metal ions (i.e., $\text{K}^+\text{H}_2\text{O}$ and K^+NH_3)^{2,49} to more strongly spatially directed interactions where electron transfer from the HOMO of the neutral to the LUMO of the ion has been suggested (i.e., Kr^+O_2 and CO_2^+CO_2).^{7,9} Two general trends for the bonding seem to emerge: (1) for bonds dominated by electrostatic forces, the bond strength is found to correlate with the ionic radius and the polarizability, the dipole moment, and the quadrupole moment of the neutral; (2) for bonds dominated by HOMO/LUMO interactions, the bond strength depends upon many factors including orbital overlap, electron density, and repulsion forces.

In the HOMO/LUMO-dominated instances the bond strength seems to increase as the difference in ionization potentials of the two neutrals decreases. The bond energies and the differences

(48) Busch, G. E.; Wilson, K. R. *J. Chem. Phys.* 1972, 56, 3626.

(49) Kebarle, P. *Annu. Rev. Phys. Chem.* 1977, 28, 445.

in ionization potentials (IP's)⁵⁰ for the two cluster moieties are presented in Table I. It is evident that the symmetric clusters (CO_2^+CO_2 and $\text{N}_2\text{O}^+\text{N}_2\text{O}$) are more strongly bound than any of the mixed clusters and that the bond energy decreases as the IP difference increases. The correlation between IP difference and bond energy is better for NO^+ and O_2^+ bound to N_2O than to CO_2 . It is clear, however, that many factors enter into the bonding picture and simple correlations for all types of ion-molecule clusters will not always be meaningful or possible.

The structures assumed in the text, d-f, are presented as reasonable molecular configurations; the author of course realizes that a definitive statement on the geometry and molecular parameters of these gas-phase cluster ions can be made only after much more experimental and/or theoretical data are available.

Acknowledgment. I thank the Auburn University Chemistry Department for partial support of this work and the Auburn University Office of Research for Grants-in-Aid 84-180, 85-190, and 87-161. I also acknowledge Mark Johnson of the Physics Instrument Shop, Carleton Nelson and Anthony Nelson of the Chemistry Glass Shop, and Frank Bowers of the Chemistry Electronics Shop for their technical support in constructing and setting up the experimental apparatus and Joe Cotrolla for writing some of the plotting software used in the data analysis.

Appendix

Statistical mechanical calculations were carried out to estimate the heat capacity corrections necessary to determine the bond dissociation energies (heat of reaction at 0 K) and the standard enthalpies and entropies of formation at 298 K. The frequencies and geometries were refined by adjusting them so that the entropies for the formation reactions (eq 13, 15-20) calculated with statistical thermodynamics⁵¹⁻⁵³ matched the experimentally

(50) Rosenstock, H. M.; Drayl, K.; Steiner, B. W.; Herron, J. T. *J. Phys. Chem. Ref. Data* 1977, 6, Suppl. 1, 1.

(51) Benson, S. W. *Thermochemical Kinetics*, 2nd ed.; Wiley: New York, 1976.

(52) McQuarrie, D. A. *Statistical Thermodynamics*; Harper & Row: New York, 1973.

(53) Davidson, N. *Statistical Mechanics*; McGraw-Hill: New York, 1962.

(54) Chase, M. W., Jr.; Davies, C. A.; Downey, J. R., Jr.; Frurip, D. J.; McDonald, R. A.; Syverud, A. N. *J. Phys. Chem. Ref. Data* 1985, 14, Suppl. 1, 1.

measured values reported in this paper.

The parameters used in the calculations for CO_2^+CO_2 are summarized in Table I. The vibrational frequencies used are very similar to those of ref 9 and 20 while the molecular geometry used for the calculation of the rotational moment of inertia was the C_{2v} geometry from the ab initio calculations in ref 9.

The parameters arrived at for the remaining clusters drew heavily on those for CO_2^+CO_2 since no ab initio data were available for these clusters. The CO_2^+CO_2 cluster ion has the strongest bond of all the clusters reported in this work (Table I); thus, slightly lower vibrational frequencies for the four new modes formed upon clustering and a slightly longer bond length between the moieties were often used for the other clusters. In all cases the parameters required for all the reactants in this paper (both neutrals and ions) are well-known and were used as reported.^{50,54}

The SO_2^+CO_2 cluster was considered to have an internal rotation which was treated as being unhindered. Its contribution to the entropy was calculated by using the reduced moment of inertia.⁵¹ Contributions to the heat capacity were considered to be classical. The reactions producing $\text{N}_2\text{O}^+\text{N}_2\text{O}$, $\text{O}_2^+\text{N}_2\text{O}$, and $\text{NO}^+\text{N}_2\text{O}$ were all found to have entropies that were less negative than those for many clustering reactions.³ It was not possible to match the experimentally measured entropies without using internal rotational degrees of freedom or extremely low vibrational degrees of freedom in the clusters. The structures indicated in the text were chosen and the parameters were found by using an unhindered rotation about the bond joining the two moieties.⁵¹ For O_2^+CO_2 and NO^+CO_2 no internal rotational degrees of freedom were required in the calculations and all internal degrees of freedom were treated as vibrations.

Although the process by which the molecular parameters were arrived at may seem arbitrary, the reader should be reminded that similar approaches have been very successfully applied to unimolecular reactions (ref 20 and references cited therein), and more important for the present application is the fact that the unknown parameters enter into the smallest terms in the heat capacity correction, which itself is a small correction to the bond dissociation energy. Thus rather than ignore the heat capacity differences of the reactants and products the corrections have been applied.

Registry No. CO_2^+CO_2 , 12693-15-1; SO_2^+CO_2 , 113859-65-7; $\text{N}_2\text{O}^+\text{N}_2\text{O}$, 80220-06-0; O_2^+CO_2 , 80094-28-6; NO^+CO_2 , 69382-81-6; $\text{O}_2^+\text{N}_2\text{O}$, 113859-66-8; NO^+NO_2 , 113892-41-4; CO_2^+ , 12181-61-2.

Micellar Effects upon Substitutions by Nucleophilic Anions

Clifford A. Bunton* and John R. Moffatt

Department of Chemistry, University of California, Santa Barbara, California 93106
(Received: September 30, 1987; In Final Form: December 14, 1987)

Micellar effects upon reactions of OH^- with *p*-nitrophenyl diphenyl phosphate or 2,4-dinitro-1-chloronaphthalene have been examined with cetyltrimethylammonium surfactants, (CTAX, X = Cl, Br, $(\text{SO}_4)_{1/2}$). Demethylations of methyl benzene- or naphthalene-2-sulfonate by halide ion have been examined in micelles of CTACl, CTABr, $\text{CTA}(\text{SO}_4)_{1/2}$, or cetyltrimethylammonium mesylate (CTAOMs) and for demethylation by OH^- or SO_3^{2-} in $\text{CTA}(\text{SO}_4)_{1/2}$ or CTAOMs. The rate enhancements have been treated in terms of concentrations of the substrates and the nucleophilic anions at the micellar surface. The anion concentrations depended upon nonspecific Coulombic and specific interactions that were calculated by solving the Poisson-Boltzmann equation. The same structural parameters were used in fitting data for reactions with Cl^- or Br^- as nucleophiles and for systems with Cl^- or Br^- as inert anions that were competing with OH^- or SO_3^{2-} . The treatment is applicable to mixtures of dilute mono- and dianions.

Ionic colloidal self-assemblies, e.g., micelles,¹ microemulsion droplets,² and vesicles,³ assist bimolecular reactions of counterions

with substrates bound to the assemblies. Increased reactant concentrations at the surfaces of the assemblies are of major